

Elucidating the Influence of Bubble Surface Area on Mass Transfer Kinetics in Gas/Liquid Systems

Anirban Ghosh¹, Michael Miranda¹, Clint P. Aichele^{1*}

¹School of Chemical Engineering, Oklahoma State University
420 Engineering North, Stillwater, OK-74078, United States

anirban.ghosh@okstate.edu; michaelangelomiranda@gmail.com; clint.aichele@okstate.edu

Abstract - The separation of gas from liquid and the hydrodynamic phenomena that govern this behaviour has numerous engineering applications, particularly in the field of hydrocarbon separations where such information is critical for designing separation equipment. In these systems, liquid is typically super-saturated with a gas under pressure, and the rate at which this gas exits the liquid is needed in order to properly predict the residence time required for separation. Several physical parameters govern the separation behaviour including the presence of bubbles, surfactants, and emulsions. This presentation specifically addresses the role that bubble surface area plays in determining the mass transfer rate of gas exiting liquids. The influence of viscosity and surface tension are also explored in the context of bubble generation. An optical technique was developed and validated to determine bubble surface area using a high-definition camera. By utilizing a unique experimental setup that facilitates the measurement of mass transfer rates at elevated pressures in conjunction with quantitative visual observations, data is obtained that reveals the connection between bubble surface area and mass transfer. Data will also be presented for systems that include surfactants, particles of varying wettability, and emulsions. The outcomes of this work will improve understanding of the processes that govern gas evolution in super-saturated conditions, thereby leading to improved designs that facilitate more efficient separation.

Keywords: Bubbling, mass transfer, separations, gas evolution, surface area, silicone oils

1. Introduction

Bubbling represents a widespread occurrence in both natural and artificial processes, finding application in various industrial applications such as ultrasound imaging, adsorption, printing technology, foaming, polymer technology, lubricating oil technology, the food industry, bioprocess engineering, and water treatment, among others (1–5). Microbial water treatment stands out as a process that relies heavily on the presence of bubbles (6). The dynamics of heat, mass, and momentum transport within a system are profoundly influenced by the bubble environment (7). If bubbles are merely carried by the liquid after the establishment of the flow pattern, they typically do not significantly alter the nature and rate of mass transfer. However, for bubbling to exert a noteworthy impact on the transport properties of a system, it is crucial that the bubbles generated significantly influence the flow field. The authors additionally emphasized the substantial role of the contact area of bubbles in determining the rate of mass transfer. To precisely quantify the volume and surface area of bubbles, a thorough understanding of the size and number of bubbles within a system is imperative.

In the oil and gas industries, effectively separating gas and liquid phases poses a significant challenge. The kinetics of gas evolution from the liquid phase is often not well comprehended, leading to two primary challenges in the separation process: gas carry under (GCU) and liquid carry over (LCO) (8,9). While numerous research works address LCU-related issues, there is a notable scarcity in addressing GCU concerns. Existing literature indicates that relying on industrial thumb rules for gas evolution estimates may lack practical accuracy in many scenarios (10,11). Preliminary investigations into GCU were conducted at atmospheric pressure, utilizing water and organic liquids as the liquid phase, with carbon dioxide and oxygen as the primary gas phases. Daniel et al. extended these tests to elevated pressures, reaching up to 1500 psia (12). The gas evolution tests, conducted at both lower and higher pressures, revealed a symmetry between gas absorption and desorption phenomena. Miranda et al. delved into gas evolution at elevated pressures to comprehend the various underlying forces involved (13). Parameters explored in the work of Miranda et al encompassed the presence of emulsions, emulsion droplet sizes, temperature, pressure, and chemical additives (14,15). Additionally, studies have been conducted to discern the impact of varying shear environments on the gas evolution process (16).

Multiphase fluids undergo diverse shear environments throughout the phase separation process, ranging from high shear rates in cyclone-type separators to low shear conditions in conventional separators (17). The presence of varying shear rates gives rise to the phenomenon of bubbling. In conventional gas-liquid separators, inlet conditioning devices such as vane-type or cyclone-type devices are commonly employed (16). Gas-liquid cylindrical cyclones (GLCCs) are also utilized for separation in the petroleum industry (18). These inlet conditioning devices and GLCCs can generate high shear rates, leading to bubbling within the separator, thereby making bubbling an integral aspect of the separation process (19). This paper aims to enhance our comprehension of gas evolution behavior by focusing on the bubbling perspective. The novelty of this work lies in establishing connections between the viscosity of a liquid, bubbling regime, supersaturation ratio, and gas evolution, thereby presenting a comprehensive view of the mass transfer process.

2. Materials and Methods

2.1. Experimental System

The current study uses silicone oils of varying viscosities manufactured by DOW chemicals. The Silicone oils share the same name XIAMETER™ PMX-200. The Viscosity of the silicone oils ranged from 1 cP to 485 cP.

High-purity methane (99.99%) from Stillwater Steel was used as the gas phase throughout this work. Spheres of known dimensions were obtained from Cospheric LLC for conducting validation tests. The properties of the polyethylene beads have been listed in the following table. All the data provided in the table has been obtained from the vendor.

2.2 Experimental Setup

The experimental configuration closely resembles the setup employed in our prior study (14), with a notable exception: the vessel is now constructed from glass. A concise overview of the setup is outlined below. The gas evolution experimental setup (see Figure 1) features a jacketed glass vessel produced by the Parr Instrument Company, having an inner diameter of 0.0914 m. This glass vessel is designed to withstand pressures of up to 150 psia and temperatures reaching 498.15 K. Equipped with a magnetically driven mixer from Parr Instrument Company, the glass vessel incorporates a 6-bladed Rushton turbine as its impeller, possessing a diameter of 0.0508 m.

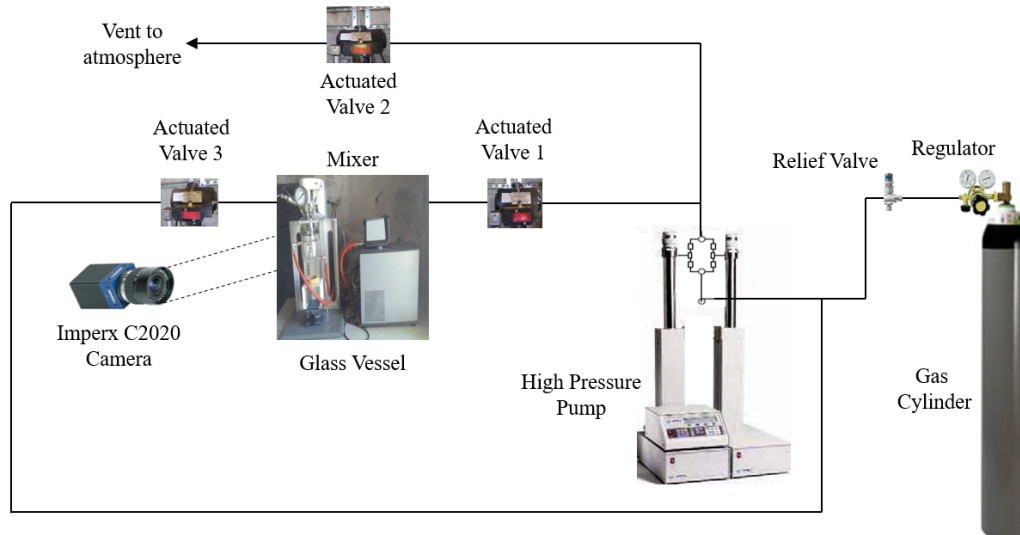


Figure 1. Schematic of the low-pressure experimental setup.

The glass vessel provides the added advantage of visualizing the experimental sample, facilitating a comprehensive understanding of fluid behaviour during the gas evolution process. This visual clarity proves instrumental in discerning bubbling behaviour, liquid swelling, and interface dynamics within the fluid matrix. Furthermore, the transparent view into the fluid matrix is instrumental in determining the mixing speed at which entrainment occurs for various fluids. To capture the gas evolution process in meticulous detail, a high-speed camera, specifically a 3.2 MP high-definition camera with a pixel size of 2064 x 1544 from Imperx, was employed. Capable of capturing up to 148 frames per second, this camera was crucial for obtaining precise insights. The images captured by the camera underwent quantitative analysis using Image J.

The experimental protocol unfolds in three main phases: absorption, depressurization, and gas evolution, a methodology consistently applied in previous articles from our research group (15,16). To ascertain the experimental uncertainty and volumetric mass transfer coefficients, established methods from prior studies within our group were utilized (15,16).

3. Results and Discussion

In order to quantify the increase in surface area resulting from bubbling, a comprehensive understanding of bubbling dynamics at different supersaturation ratios was imperative. Notably, our observations indicated the absence of bubbling during the gas absorption phase. Representative images during the gas evolution process for fluids exhibiting different viscosities at supersaturation ratios of 0.3 and 3 are illustrated in Figures 2 and 3.

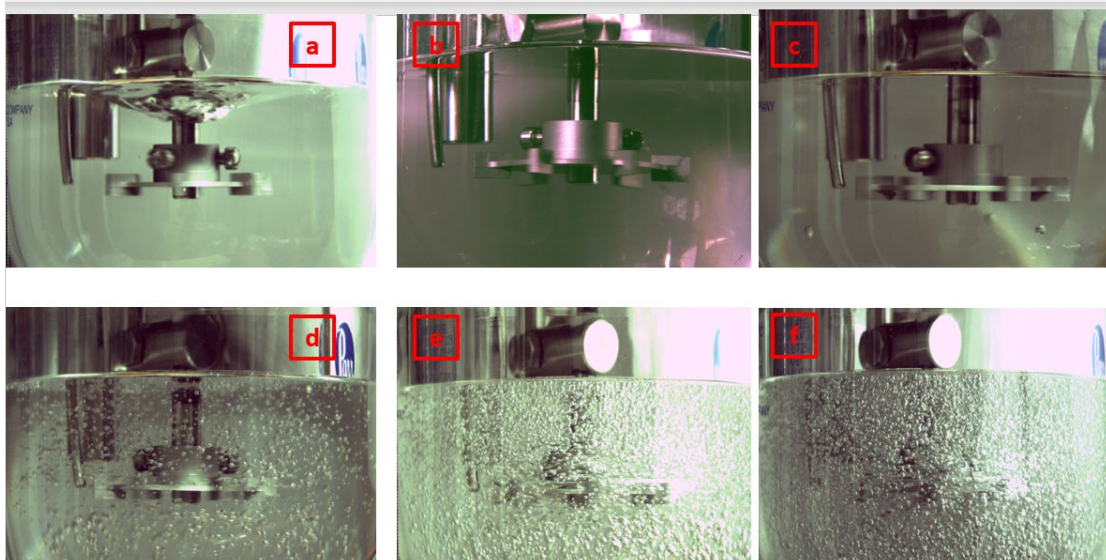


Figure 2. Representative image for gas evolution from silicone oils at 250 RPM and a supersaturation ratio of 0.3, (a) 0.82 cP, (b) 48 cP, (c) 96.4 cP, (d) 194 cP, (e) 339.15 & (f) 485 cP.

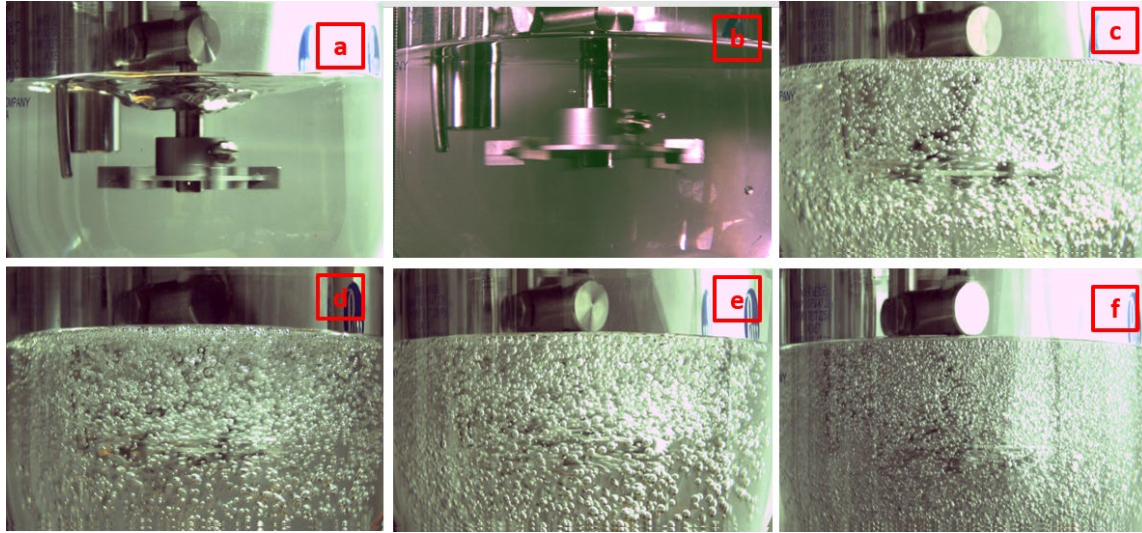


Figure 3. Representative image for gas evolution from silicone oils at 250 RPM and a Supersaturation ratio of 3, (a) 0.82 cP, (b) 48 cP, (c) 96.4 cP, (d) 194 cP, (e) 339.15 & (f) 485 cP.

Figures 2 and 3 reveal the different regimes of bubbling that may be encountered during the process of gas evolution with a varied range of viscous fluids.

3.1 Quantifying the Contribution of the Surface Area Toward Mass Transfer

The calculations and inferences concerning the correlation between the rate of mass transfer and the bubbling process were derived using the following six equations. Specifically, Equation 2 characterizes a perfectly mixed gas-liquid contactor.

$$\frac{dC}{dt} = k_L a (C^* - C) \quad (\text{Eq. 2})$$

Integrating $\ln\left(\frac{C - C^*}{C_0 - C^*}\right) = k_L a t$ (Eq. 3)

$$(a)_{\text{absorption}} = \frac{A_i}{V} \quad (\text{Eq. 4})$$

$$(a)_{\text{gas evolution}} = \frac{A_i + A_B}{V} \quad (\text{Eq. 5})$$

The ratio of gas evolution as compared to absorption

$$= \frac{(k_L a)_{\text{gas evolution}}}{(k_L a)_{\text{absorption}}} \quad (\text{Eq. 6})$$

$$\frac{(a)_{\text{gas evolution}}}{(a)_{\text{absorption}}} = \frac{\frac{A_i + A_B}{V}}{\frac{A_i}{V}} = \frac{A_i + A_B}{A_i} \quad (\text{Eq. 7})$$

where:

k_L = mass transfer coefficient (m/s), C^* = final equilibrium gas concentration (mol/L), a = specific surface area (m^{-1}), A_i = interfacial area for mass transfer (m^2), A_B = surface area due to bubbles, V = liquid volume (m^3).

Equations 2 and 3 serve as the governing expressions for mass transfer in our system. In instances where gas evolution occurs alongside nucleation, the value of $k_L a$ for gas evolution exceeds that of gas absorption. Equations 4 and 5

define the specific surface area calculated for absorption and gas evolution, respectively. $\frac{(k_L a)_{\text{gas evolution}}}{(k_L a)_{\text{absorption}}}$ and $\frac{(a)_{\text{gas evolution}}}{(a)_{\text{absorption}}}$ have been defined to compare the contribution of nucleation to mass transfer coefficient in equations 6 and 7, respectively. Equation 6 delineates the ratio of volumetric mass transfer coefficients for gas evolution and gas absorption. This ratio provides insights into the comparative efficiency of mass transfer between the two processes. On the other hand, Equation 7 quantifies the ratio of available surface area during mass transfer for gas evolution in relation to that of gas absorption. This ratio elucidates how the surface area utilization differs between the two phases of the process, offering valuable information about the impact of bubbling on mass transfer dynamics.

The initial step in comprehending the contribution of bubbles to accelerating the rate of mass transfer involves understanding the gas evolution process. Figure 4 provides a visual representation of the comparison between the volumetric mass transfer coefficients for gas absorption and gas evolution. This comparative analysis sheds light on how the mass transfer efficiency varies between the two processes, offering a crucial foundation for assessing the role of bubbling in influencing the rate of mass transfer. This ratio of comparison is essentially $\frac{(k_L a)_{\text{gas evolution}}}{(k_L a)_{\text{absorption}}}$ as defined by equation 6. It can be seen from figure 4 that the $\frac{(k_L a)_{\text{gas evolution}}}{(k_L a)_{\text{absorption}}}$ increases drastically for the cases of mixing speed 250 RPM and supersaturation ratio 3, which is also reflected in figure 5. An increase in the values of $\frac{(k_L a)_{\text{gas evolution}}}{(k_L a)_{\text{absorption}}}$ can also be noticed for the 339cP and 485cP oils at a mixing speed of 250 RPM and supersaturation ratio of 0.3, both from figure 4. The value for the ratio $\frac{(k_L a)_{\text{gas evolution}}}{(k_L a)_{\text{absorption}}}$ at a supersaturation ratio of 0.3 for the 96.4 cP and 194 cP silicone oil is 1. This value is also justified by the visual observations reflected in figure 3, which shows that there was no bubbling during gas evolution from the 96.4 cP silicone oil while there was minimal bubbling from the 194 cP silicone oil.

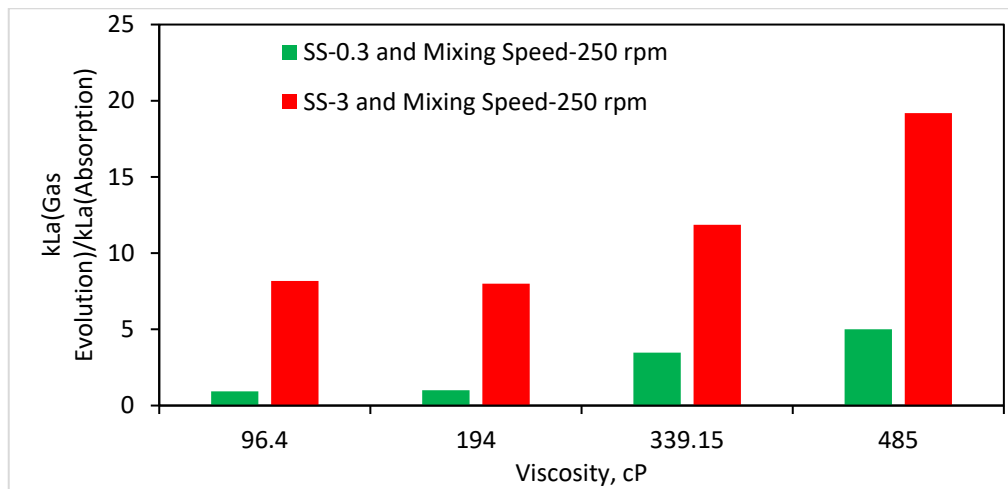


Figure 4. Comparison of the rate of gas evolution to the rate of gas absorption.

Figure 5 shows the values of $\frac{(k_L a)_{\text{gas evolution}}}{(k_L a)_{\text{absorption}}}$ and $\frac{(a)_{\text{gas evolution}}}{(a)_{\text{absorption}}}$ evaluated for the high-bubbling fluids at a supersaturation ratio of 0.3. The experiments were all conducted at a mixing speed of 250 RPM. The $\frac{(a)_{\text{gas evolution}}}{(a)_{\text{absorption}}}$ and $\frac{(k_L a)_{\text{gas evolution}}}{(k_L a)_{\text{absorption}}}$ values rise in tandem with each other till the 485 cP viscosity mark. This agreement between the two ratios reflects the effect of the additional surface area due to bubbling may be directly related to an increase in the rate of mass

transfer. This may explain the fact that when the liquid viscosity gets higher the gas evolution process takes place at a very enhanced rate at the beginning of the process.

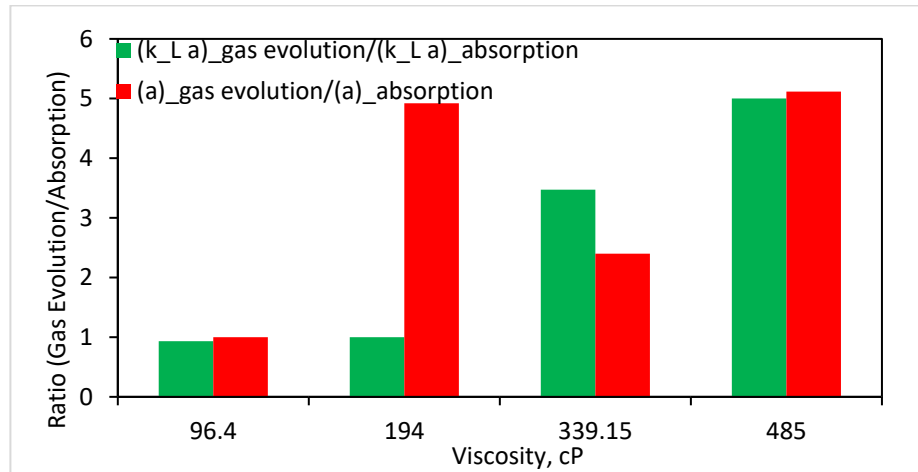


Figure 5. Comparison of the rate of gas evolution to the rate of gas absorption (SSR=0.3).

Figure 6 shows the values of $\frac{(k_L a)_{\text{gas evolution}}}{(k_L a)_{\text{absorption}}}$ and $\frac{(a)_{\text{gas evolution}}}{(a)_{\text{absorption}}}$ evaluated for the high-bubbling fluids at a supersaturation ratio of 3. The experiments were all conducted at a mixing speed of 250 RPM. The figure provides some interesting insights into the rate of gas evolution at elevated supersaturation ratios from the perspective of nucleation. The value of $\frac{(k_L a)_{\text{gas evolution}}}{(k_L a)_{\text{absorption}}}$ for the 96.4 cP liquid is comparable to the respective value of the ratio $\frac{(a)_{\text{gas evolution}}}{(a)_{\text{absorption}}}$. In the case of the 194 cP silicone oil the values for $\frac{(k_L a)_{\text{gas evolution}}}{(k_L a)_{\text{absorption}}}$ is lesser in value when compared to the $\frac{(a)_{\text{gas evolution}}}{(a)_{\text{absorption}}}$ value behaviour of the histogram changes again with the increase in viscosity. The value of $\frac{(k_L a)_{\text{gas evolution}}}{(k_L a)_{\text{absorption}}}$ gradually catches up with the value of $\frac{(a)_{\text{gas evolution}}}{(a)_{\text{absorption}}}$.

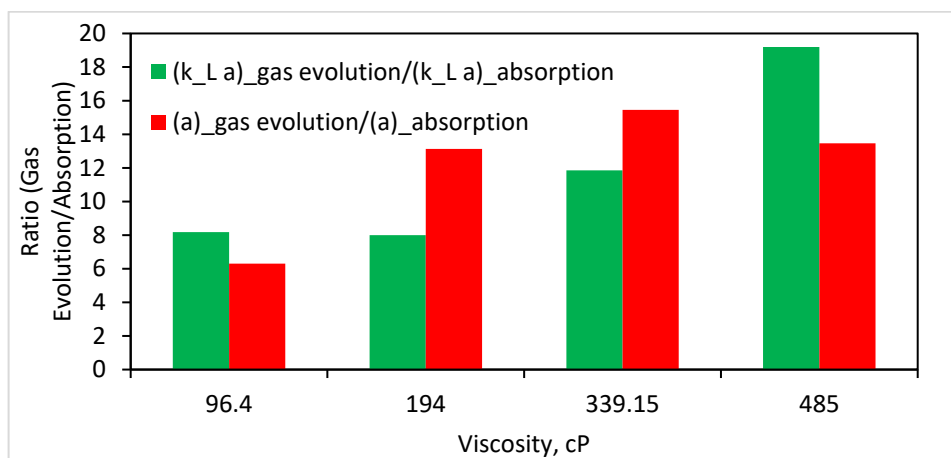


Figure 6. Comparison of the rate of gas evolution to the rate of gas absorption (SSR=3).

The trend of $\frac{(k_L a)_{\text{gas evolution}}}{(k_L a)_{\text{absorption}}}$ falling behind $\frac{(a)_{\text{gas evolution}}}{(a)_{\text{absorption}}}$ with the increase in viscosity and supersaturation ratio and later catching up with $\frac{(a)_{\text{gas evolution}}}{(a)_{\text{absorption}}}$ needs explanation. The following section intends to explain this behaviour.

4. Conclusions

The evaluation of surface area for three different regimes was conducted using an image-based technique. Notably, bubbling was not observed in the liquid matrix at speeds below 250 RPM, and no bubbling occurred with liquids having a viscosity of less than 96 cP. A comparative analysis was performed to assess the relationship between the increase in surface area and the rate of gas evolution. The study explored the contribution of excess surface area to the mass transfer rate, revealing that an increase in surface area correlated with an enhanced mass transfer rate. This study challenges conventional understanding, suggesting that, contrary to previous notions, higher viscosity fluids with bubbling evolve gas faster than lower viscosity fluids under similar experimental conditions. Simultaneously, it was observed that the process of gas evolution can progress much more rapidly for fluids with high viscosity, contingent upon the energy input during gas evolution. The findings of this work suggest the possibility of determining the rate of gas evolution based on the bubbling behavior and viscosity of the fluid. Ultimately, this research underscores the interconnected role of viscosity, supersaturation ratio, and bubble surface area in influencing the mass transfer rate.

Acknowledgements

We thank the Fluid Phase Kinetics Joint Industry Project for funding this work. We also thank Norman Yeh and Alden Daniel for their insightful contributions.

References

- [1] Patel AK, Singhanian RR, Chen CW, Tseng YS, Kuo CH, Wu CH, Dong CD. Advances in micro- and nano bubbles technology for application in biochemical processes. *Environmental Technology & Innovation*. 2021 Aug;23:101729.
- [2] Jia Y, Wang R, Fane A. Atrazine adsorption from aqueous solution using powdered activated carbon—Improved mass transfer by air bubbling agitation. *Chemical Engineering Journal*. 2005 Dec 13;S1385894705004110.
- [3] De Jong J, Jeurissen R, Borel H, van den Berg M, Wijshoff H, Reinten H, Versluis, M, Prosperetti A, Lohse D. Entrapped air bubbles in piezo-driven inkjet printing: Their effect on the droplet velocity. *Physics of Fluids*. 2006 Dec;18(12):121511.
- [4] Chandran Suja V, Kar A, Cates W, Remmert SM, Savage PD, Fuller GG. Evaporation-induced foam stabilization in lubricating oils. *Proc Natl Acad Sci USA*. 2018 Jul 31;115(31):7919–24.
- [5] Chandran Suja V, Kar A, Cates W, Remmert SM, Fuller GG. Foam stability in filtered lubricants containing antifoams. *Journal of Colloid and Interface Science*. 2020 May;567:1–9.
- [6] DeMoyer CD, Schierholz EL, Gulliver JS, Wilhelms SC. Impact of bubble and free surface oxygen transfer on diffused aeration systems. *Water Research*. 2003 Apr;37(8):1890–904.
- [7] Mei, Zhongkai, and Xu Cheng. "Impact of bubble dynamics on aerosol transport based on CFD analysis." *Progress in Nuclear Energy* 161 (2023): 104723.
- [8] Lavenson DM, Kelkar AV, Daniel AB, Mohammad SA, Kouba G, Aichele CP. Gas evolution rates – A critical uncertainty in challenged gas-liquid separations. *Journal of Petroleum Science and Engineering*. 2016 Nov;147:816–28.
- [9] Lavenson DM, Kelkar AV, Joshi N, Portman L. Kinetics of Fluid Phase Behavior Changes: A Critical Uncertainty for Offshore Field Development. In: Day 3 Wed, May 03, 2017
- [10] Bothamley M. Gas/Liquid Separators: Quantifying Separation Performance - Part 1. *Oil and Gas Facilities*. 2013 Aug 1;2(04):21–9.
- [11] Bothamley M. Gas/Liquids Separators: Quantifying Separation Performance - Part 3. *Oil and Gas Facilities*. 2013 Dec 1;2(06):34–47.

- [12] Daniel AB, Mohammad SA, Miranda MA, Aichele CP. Absorption and desorption mass transfer rates as a function of pressure and mixing in a simple hydrocarbon system. *Chemical Engineering Research and Design*. 2019 Apr;144:209–15.
- [13] Miranda MA, Subramani HJ, Aichele CP. Impact of Supersaturation Ratio on the Kinetics of Gas Evolution at Elevated Pressures. *Energy Fuels*. 2020 Dec 17;34(12):15812–8.
- [14] Miranda MA, Yegya Raman AK, Lavenson DM, Subramani HJ, Mohammad SA, Aichele CP. Gas Evolution Rates in Supersaturated Water-in-Oil Emulsions at Elevated Pressures. *Energy Fuels*. 2019 Sep 19;33(9):8176–83.
- [15] Miranda MA, Yegya Raman AK, Mohammad SA, Subramani HJ, Aichele CP. Impact of Chemical Additives on Gas Evolution Behavior in Supersaturated Solutions at Elevated Pressures. *Energy Fuels*. 2021 Jun 17;35(12):9894–902.
- [16] Miranda MA, Ghosh A, Yegya Raman AK, Subramani HJ, Mohammad SA, Aichele CP. A Predictive Methodology to Determine the Rate of Gas Evolution in Hydrocarbon Systems at Elevated Pressures. *Energy Fuels*. 2023 Jun 1;37(11):7657–66.
- [17] Chirinos WA, Gomez LE, Wang S, Mohan R, Shoham O, Kouba G. Liquid Carry-over in Gas-Liquid Cylindrical Cyclone Compact Separators. In Houston, Texas: SPE; 1999 [cited 2021 Oct 28]. p. SPE-56582-MS
- [18] Kouba G, Shoham O. A review of gas-liquid cylindrical cyclone (glcc) technology. In Citeseer; 1996. p. 23–4.
- [19] Hreiz R, Lainé R, Wu J, Lemaitre C, Gentric C, Fünfschilling D. On the effect of the nozzle design on the performances of gas–liquid cylindrical cyclone separators. *International Journal of Multiphase Flow*. 2014 Jan;58:15–26.